frontiers | Frontiers in Ecology and Evolution

ORIGINAL RESEARCH
published: 24 June 2022
doi: 10.3389/fevo.2022.900544

Rapid Shifts in Visible Carolina Grasshopper (*Dissosteira carolina*) Coloration During Flights

*Ezekiel Martin, Henry L. Steinmetz, Seo Young Baek, Frederick R. Gilbert and Nicholas C. Brandley**

Department of Biology, The College of Wooster, Wooster, OH, United States

Some brightly colored structures are only visible when organisms are moving, such as parts of wings that are only visible in flight. For example, the primarily brown Carolina grasshopper (*Dissosteira carolina*) has contrasting black-and-cream hindwings that appear suddenly when it takes off, then oscillate unpredictably throughout the main flight before disappearing rapidly upon landing. However, the temporal dynamics of hindwing coloration in motion have not previously been investigated, particularly for animals that differ from humans in their temporal vision. To examine how quickly this coloration appears to a variety of non-human observers, we took high-speed videos of *D. carolina* flights in the field. For each of the best-quality takeoffs and landings, we performed a frame-by-frame analysis on how the relative sizes of the different-colored body parts changed over time. We found that in the first 7.6 ± 1.5 ms of takeoff, the hindwings unfurled to encompass 50% of the visible grasshopper, causing it to roughly double in size. During the main flight, the hindwings transitioned 6.4 ± 0.4 times per second between pauses and periods of active wing-beating (31.4 ± 0.5 Hz), creating an unstable, confusing image. Finally, during landings, the hindwings disappeared in 11.3 ± 3.0 ms, shrinking the grasshopper to 69 ± 9% of its main flight size. Notably, these takeoffs and landings occurred faster than most recorded species are able to sample images, which suggests that they would be near-instantaneous to a variety of different viewers. We therefore suggest that *D. carolina* uses its hindwings to initially startle predators (deimatic defense) and then confuse them and disrupt their search images (protean defense) before rapidly returning to crypsis.

Keywords: orthoptera, Oedipodinae, deimatic defense, protean defense, crypsis, critical flicker fusion, temporal vision

OPEN ACCESS

Edited by:
Eunice Jingmei Tan,
Yale-NUS College, Singapore

Reviewed by:
Katja Rönkä,
University of Helsinki, Finland
Amanda Franklin,
The University of Melbourne, Australia

***Correspondence:**
Nicholas C. Brandley
nbrandley@wooster.edu

Specialty section:
This article was submitted to Behavioral and Evolutionary Ecology, a section of the journal Frontiers in Ecology and Evolution

Received: *20 March 2022*
Accepted: *23 May 2022*
Published: *24 June 2022*

Citation:
Martin E, Steinmetz HL, Baek SY, Gilbert FR and Brandley NC (2022) Rapid Shifts in Visible Carolina Grasshopper (Dissosteira carolina) Coloration During Flights. Front. Ecol. Evol. 10:900544. doi: 10.3389/fevo.2022.900544

INTRODUCTION

Most animals' surroundings are full of motion, and therefore the ability to perceive moving stimuli may play a large role in their evolutionary success (Tan and Elgar, 2021). For example, movement can enhance visual signals (Peters et al., 2007; Ord and Stamps, 2008), reveal prey to predators (Ioannou and Krause, 2009; Hall et al., 2013), or be used to confuse predators once prey are detected (Maldonado, 1970; How and Zanker, 2014; Umbers et al., 2015; Ruxton et al., 2018; Murali et al., 2019). Yet in many cases, studies of animal appearances focus on static scenes, limiting our knowledge of how they may function in a moving world.

The motion of patterns is further complicated when they change over time. In these cases, it is not solely movement that matters, but the temporal changes in the stimulus. For example,

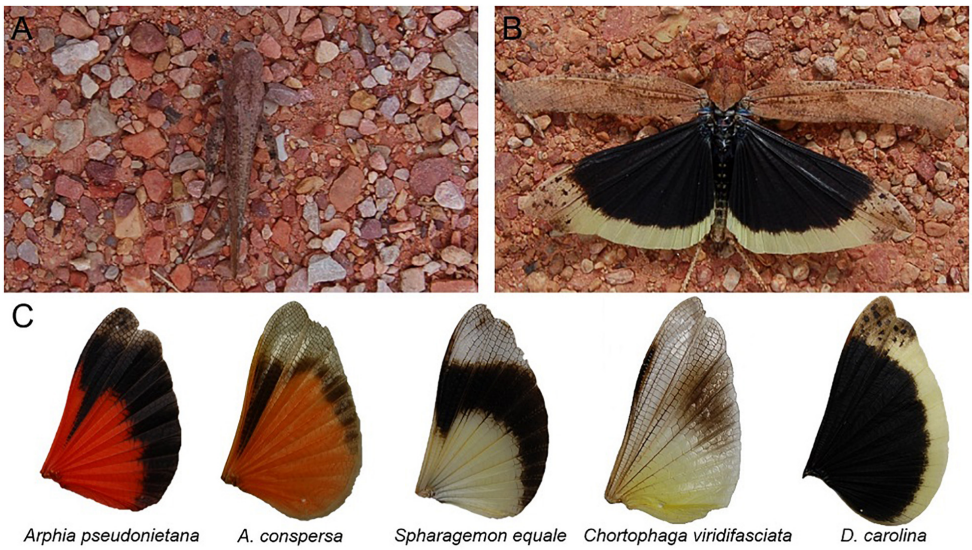

FIGURE 1 | The of band-winged grasshoppers are revealed in flight. **(A)** When at rest the Carolina grasshopper's (*Dissosteira carolina*) main body coloration often matches the environment, rendering it cryptic. **(B)** A posed grasshopper shows the conspicuous and high-contrast hindwings that are unveiled during flight. **(C)** Hindwing patterning is variable across species including in color, location and size of the black band, and transparency. Proper understanding of this patterning requires accounting for its motion and temporal dynamics.

some cephalopods actively produce a "passing cloud" appearance (Mather and Mather, 2004; Laan et al., 2014), male peacock spiders unfurl their colorful opisthosomal flaps before signaling (Girard et al., 2011), and some butterflies transition between camouflage and conspicuous eye spots by showing different sides of their wings (Vallin et al., 2005; Olofsson et al., 2013). In each case, these behaviors may depend both on movement and on the changes between appearances.

Band-winged grasshoppers (subfamily Oedipodinae) present an interesting case study on movement and changing appearances because of the variety of patterns found on their hindwings (**Figure 1**; Otte, 1985; Cooper, 2006). In most species, these hindwings include regions of black which to a human observer contrast sharply against neighboring yellow, orange, or red regions. Notably, the hindwings are hidden when the grasshopper is on the ground but are suddenly unfurled in flight (**Figure 1**). To a human observer, the hindwings appear to visually facilitate escape through three separate mechanisms. First, the initial change from camouflage to bright and contrasting coloration may startle a potential predator in a process known as a deimatic defense (Maldonado, 1970). Second, during flight, the grasshopper's appearance changes depending on whether it is gliding or actively flapping its wings (and thus causing its colors to fuse together *via* the flicker-fusion effect; Jackson et al., 1976; Umeton et al., 2017). Thus, movement of the wings in flight may disrupt a predator's search image *via* protean defense or dynamic flash coloration (Humphries and Driver, 1970; Murali, 2018). Third, when landing, the grasshopper transitions back to camouflage so quickly that researchers have "often incorrectly guessed the landing locations of . . . grasshoppers due to their sudden disappearance" (Cooper, 2006). Taken all together, transitions in grasshopper appearance could allow them to initially startle predators, then make tracking difficult, and ultimately disappear back into camouflage.

However, modern sensory biology revolves around umwelt—the idea that each species, perhaps even each organism, perceives its surroundings differently—and therefore one cannot understand the defensive function of grasshopper coloration in flight without considering the views of relevant predators. Ideally, one should account for both behavioral differences (e.g., distance and angle of view) and physiological differences (e.g., color vision and visual acuity). Notably, when discussing grasshopper coloration in motion, we need to account for their predators' temporal vision—how quickly their visual systems form images. Temporal vision is often measured using critical flicker fusion (CFF), which is the frequency necessary for flickers in light to be perceived (or, in the case of non-human animals, reacted to) as identical to a constant light with a light level midway between the on and off states of the actual, flickering light (Donner, 2021). Many species of North American band-winged grasshoppers are preyed on primarily by passerine birds (Belovsky and Slade, 1993). Passerines specialized in catching aerial insects may have temporal vision that is twice as fast as humans' (e.g., ∼120 Hz vs. ∼60 Hz; Brundrett, 1974; Boström et al., 2016), which would halve their integration times (the time required for their visual systems to form images). Therefore, to account for differences in predatory temporal umwelts, we must measure the speeds at which band-winged grasshopper coloration changes.

Here, to begin to understand the temporal mechanics of band-winged grasshopper appearance, we used high-speed video to examine the escape flights of one species of band-winged grasshopper, the Carolina grasshopper (*Dissosteira carolina*). First, we visually modeled how avian predators would view the

color and spatial aspects of a stationary grasshopper hindwing. We then filmed grasshopper flights in the field, before analyzing the highest quality footage of (1) takeoff, (2) main flight, and (3) landing. In each case, we analyzed videos frame-by-frame to understand how *D. carolina's* coloration changes, and ultimately account for differences in predator temporal vision.

MATERIALS AND METHODS

Stationary Coloration and Pattern Modeling

Dissosteira carolina (n = 51) were collected on private property between July and September of 2019. Collection occurred in one suburban site with both grassy and gravelly areas in Wayne County, OH, and one rural site consisting of a network of secluded, grassy fields and paths in Holmes County, OH. Prior to reflectance measurements, grasshoppers were euthanized *via* freezing for around 1 h. Reflectance of various grasshopper body parts (body, cream band of the hindwing, black region of the hindwing) was measured in OceanView with a spectrometer (model: FLAME-S-UV-VIS) combined with a 600-μm fiber optic probe, a PX-2 UV-visible light source, and a WS-1 diffuse reflectance standard (all Ocean Optics, Inc., Dunedin, FL, United States). The light source was directed from above, and the probe was held in place by clamps ∼1 cm from the surface at an angle of 45°.

To model how potential avian predators would view these colors, unweighted Euclidean color distances and achromatic contrasts were modeled using the pavo package (Maia et al., 2019) in R. Spectrums (300–700 nm) were first processed *via* the procspec function with a loess smoothing coefficient of 0.1 and negative values set to zero. Relative quantum catches for each photoreceptor class of a blue tit's visual system (including the achromatic double cone; Vorobyev et al., 1998; Hart, 2001) were calculated using the default vismodel function settings (ideal lighting setting, quantum catch is for each photoreceptor and not transformed, no von Kries correction). Values were then transformed into tetrahedral avian color space *via* the colspec function (Stoddard and Prum, 2008), before unweighted Euclidean color distances and achromatic contrasts were calculated *via* the coldist function (noise = neural).

To understand the maximum distance at which avian predators could fully resolve the spatial aspects of hindwing patterning, images of stationary and fully extended *D. carolina* hindwings (n = 38; courtesy of Brae Salazar) were measured in ImageJ (Schneider et al., 2012). We first identified the midpoint of the black region of the hindwing, before measuring the width of the cream band at the vein nearest to this midpoint. We then calculated the maximum distance at which the cream band could be fully resolved by an avian predator with a visual acuity of 10 cycles per degree (minimum resolvable angle = 0.05°) *via* the equation:

$$maximum\ distance = \frac{width\ of\ cream\ band}{tan(0.05°)}$$

Video Study Organisms and Site

Adult *D. carolina* were located in the same two sites as those used for the stationary color measurements. Filming took place on most days between July 19th and September 4th, 2021, and was limited to primarily sunny days without strong winds.

Video Gathering and Categorization

Videos were usually taken in a 1–2-h session each day between the hours of 11 AM and 2 PM. Videos (n = 386) were taken at 480 frames per second (fps; with an average shot length of 3.67 s) using a Sony RX100 VI HFR camera (Sony Group Corporation, Minato City, Tokyo, Japan). For each video, while filming, we briskly approached a targeted grasshopper, and then followed it if necessary. To maximize video clarity, a variety of techniques were implemented based on the circumstances of individual shots. For example, when conditions allowed, the filmer would crouch and hold the camera just below the knees to get closer to the grasshopper. To obtain landing shots in cases where subjects were unusually reactive to an approach, the filmer would sometimes use the zoom function and a longer focus to simulate a shorter distance to the subject. In other cases, subjects would be unusually latent to react and refrain from flying away during approach; in these cases, the filmer would approach more slowly (from behind, when possible), and quicken their pace once distance to target was within a yard or so. Regardless of technique, grasshoppers were typically located *via* an initial flight, so the recorded flights usually represented the second or third flight in a sequence.

D. carolina may cover tens of meters in a single flight, so analysis required prioritizing segments of flights to ensure quality footage. Of the 386 initial videos, the highest-quality takeoffs (n = 8; average max grasshopper size = 381 pixels), in-flight videos (n = 14), and landings (n = 8; average max grasshopper size = 478 pixels) were selected for frame-by-frame analysis (see below). These videos were chosen based on focus, lack of obstruction, and distance to the grasshopper.

Takeoff Frame-by-Frame Analysis

For each takeoff video (n = 8), we scored how the visible body parts—and thus coloration—of the grasshopper changed over the course of takeoff. To obtain these measurements, 120 frames (0.25 s) from each video were downloaded in R one image at a time using the packages ggplot2 (Wickham, 2016) and imager (Barthelmé and Tschumperlé, 2019) and then analyzed in ImageJ (Schneider et al., 2012). Three coloration categories were used:

(1) "brown," encompassing all visible pixels of the forewings and brown regions of the body of the grasshopper (primarily the head and hindmost section of the abdomen; see **Figure 1**) but excluding the legs, which were too thin and indistinct to be accurately measured,
(2) "black," encompassing all visible pixels of the black portion of the grasshopper's hindwings and the small black region between the hindwings, and
(3) "cream," encompassing all visible pixels of the cream fringe of the grasshopper's hindwings.

For each frame, we measured the size (in pixels) of the three different color regions using the freehand selection tool in ImageJ. In cases where a frame contained multiple separate shapes of the same color, these shapes were measured separately, then added together. Each color category was measured twice for each frame, and all measurements were only observed after a frame was fully processed. We then averaged the pairs of measurements into single values and converted them to percentages based on the combined values of all three regions. To ensure accurate measurements, four different accuracy checks were implemented throughout this process (**Supplemental Information**).

For each video, we measured the speed of transition between camouflage and conspicuousness in two different ways: (1) the time elapsed between the last fully brown frame and the first frame where brown and hindwings were equally visible or (2) the time elapsed between the last fully brown frame and the first frame where black and cream decreased in size (indicating the beginning of main flight oscillation).

Main Flight Wingbeat Frequencies

Because of the length and distance of flights, extended main flight footage was not suitable for the same frame-by-frame analysis used for take-offs. Instead, to understand how wing movement affects visible coloration during the main flight, we scored each wingbeat at the point where the wings were lowest in their flight cycle. Video quality allowed us to do this for most of the flight, though the landings were excluded. Two scorers independently viewed each video (n = 14 videos) and recorded the frames in which wingbeats occurred. We then reconciled this data by either (1) averaging the results if they were within five frames (10 ms) of each other or (2) for larger differences, reviewing the videos together, and revising the scores. In the rare cases where one viewer scored a wingbeat that the other did not, videos were reviewed together to make a final determination.

Because *D. carolina* flight alternates between periods of active wing-beating and pauses, wingbeat frequency was calculated only within a cluster of active wingbeats, but the alternating periods of activity and pauses were also recorded. We classified pauses between wingbeats based on their duration. Values $\geq$ 0.05 s but $<$ 0.1 s were classified as skips as they typically corresponded to one to two skipped wingbeats. Additionally, values $\geq$ 0.1 s but $<$ 0.25 s were classified as short glides, while values $\geq$ 0.25 s were classified as long glides.

Landing Frame-by-Frame Analysis

Procedures for landings (n = 8 videos) resembled those for takeoffs, with the last 120 frames (0.25 s) of flight being used instead. The speed of return to camouflage during landing was recorded as either (1) the time elapsed between the first frame of over 50% brown and the first fully brown frame or (2) the time elapsed between the end of the main flight oscillation (as measured for takeoffs) and the first fully brown frame.

Comparative Temporal Visual Models of Takeoff and Landing

For each takeoff or landing video, we modeled how the percent colorations of the wings would change to viewers with differing critical flicker fusions (CFF). These values included 240 Hz (used as an effective upper limit, above all known values), 120 Hz (approximate for specialized passerine predators; Boström et al., 2016), and 60 Hz (approximate for humans and non-specialist birds; Brundrett, 1974; Healy et al., 2013). In these models, the color percentages were averaged over an increasingly large number of frames, mimicking how visual stimuli occurring at a higher frequency than the viewer's CFF fuse together into a single blur. Because our videos were shot at 480 fps, for the 240 Hz CFF model, the average included the central frame and a half-weight of the frames on either side. Similarly, the averages for the 120 Hz model included the central frame, the frames on either side of it, and a half-weight of the frames on either side of those; and those for the 60 Hz model included the central frame, the three frames on either side of it, and a half-weight of the frames on either side of those.

Finally, we obtained the 90th and 10th percentiles for each color using the = PERCENTILE.INC function in Excel. Because most colors varied within this range for each video, these percentiles helped us better understand how colors oscillated in each CFF model. Values examined started from the first hindwing maximum and ended at the last frame able to be accurately measured in 60 Hz vision (frame 117).

RESULTS

Stationary Color and Pattern Modeling

Avian visual modeling shows that the black and cream regions of the hindwing contrast both chromatically and achromatically with each other (**Figure 2**, mean unweighted Euclidean color distance = 0.23 $\pm$ 0.004 SEM, mean Weber contrast = 11.62 $\pm$ 0.93). Both regions also contrast with the brown of the body, although to a lesser degree (body vs. black of hindwing Euclidean color distance = 0.19 $\pm$ 0.009, Weber contrast = 5.34 $\pm$ 0.59; body vs. cream band Euclidean color distance = 0.11 $\pm$ 0.004, Weber contrast = 1.17 $\pm$ 0.08).

In a stationary, fully extended hindwing, the cream band had an average width of 3.9 $\pm$ 0.1 mm, meaning that its spatial characteristics should be fully resolvable by a bird with a visual acuity of 10 cycles per degree at a distance of $\sim$4.5 m.

Takeoff

Each takeoff consisted of a rapid transition to a contrasting appearance (time to 50% of the viewable grasshopper being the hindwings = 7.6 ms $\pm$ 1.5, **Figures 3A,B** and **Table 1**) with a corresponding sudden doubling in grasshopper size (relative size at 50% of the viewable grasshopper being the hindwings = 2.0 $\pm$ 0.3; **Figures 3C,D** and **Table 1**). This initial burst was followed by erratic periods of visible color change during the first $\sim$0.25 s of flight (**Figures 3A,B**), with all three color regions varying temporally in their relative contributions (**Table 1**).

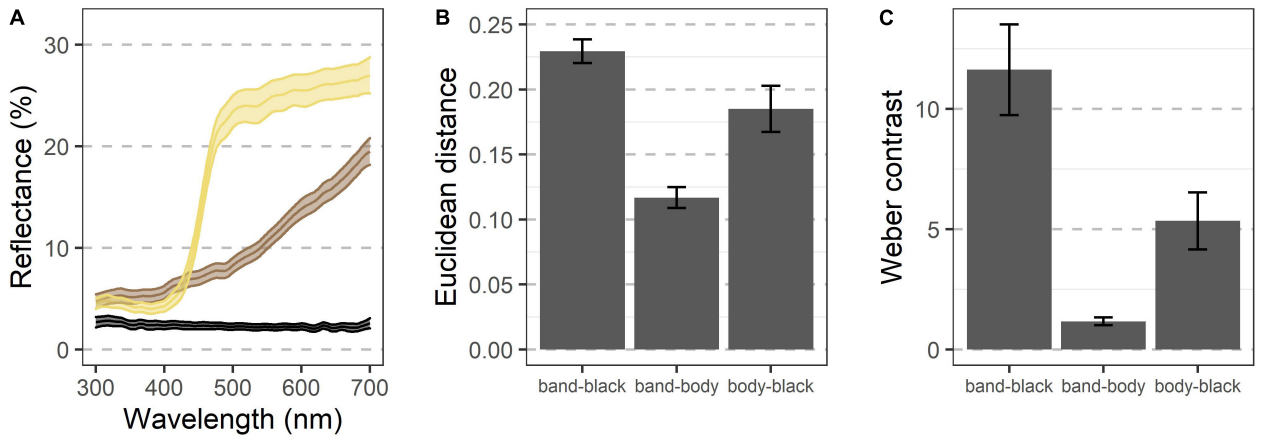

FIGURE 2 | Visual modeling indicates that the various color regions of *D. carolina* contrast both chromatically and achromatically when seen by an avian predator. **(A)** Reflectance of various regions shows diverging patterns, especially above ~425 nm (n = 51 grasshoppers). Colors indicate regions of three different appearances, including the cream band of the hindwings, the black regions of the hindwings, and the brown regions of most of the rest of the body (see text). Ribbons indicate the 95% confidence interval. **(B,C)** When modeled through the visual system of a blue tit, the regions contrast against each other both chromatically **(B)** and achromatically **(C)**, with the cream band and black of the hindwings showing the greatest contrast. Error bars indicate the 95% confidence interval.

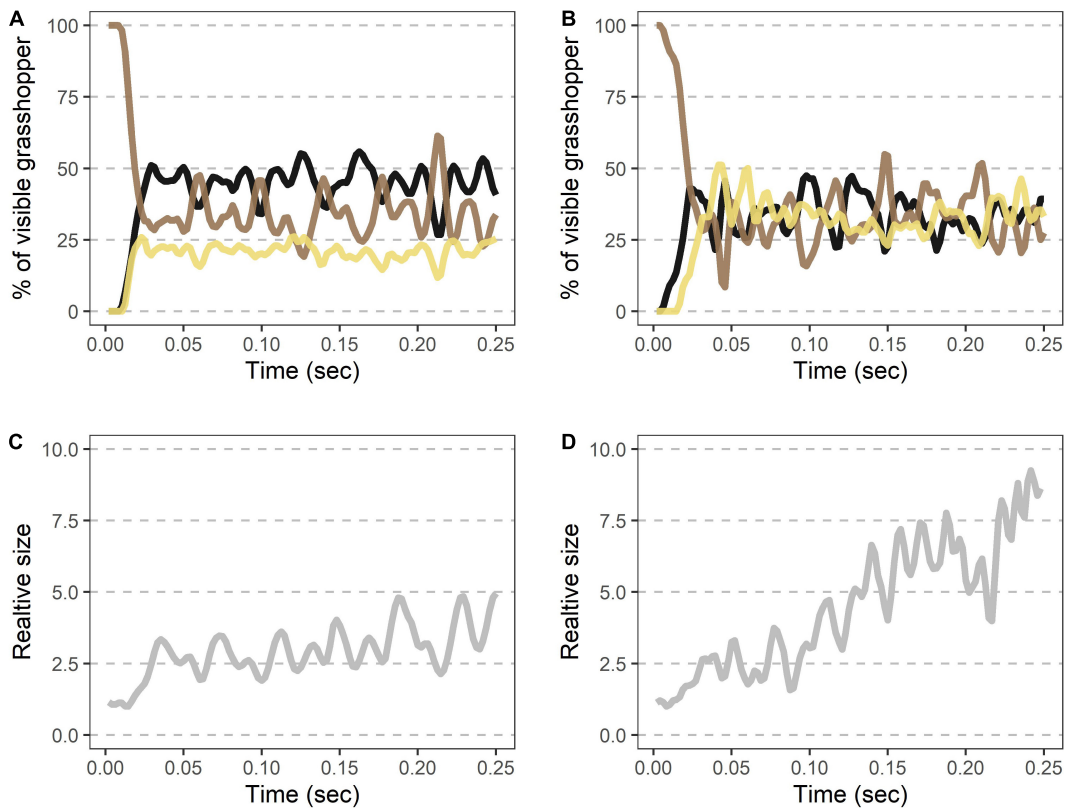

FIGURE 3 | Rapid shifts in visible color regions and size during Carolina grasshopper takeoffs. **(A,B)** Example takeoffs of two different flights show rapid but differing changes in visible coloration and size. Percent of the visible grasshopper consists of the three color categories brown, black, and cream. In each case, there is (1) a quick transition from a brown, resting grasshopper to a hindwing display (average time to 50% of the viewable grasshopper being hindwings = 7.6 ms ± 1.5 SEM), followed by (2) oscillation of visible coloration. **(A)** represents a more typical grasshopper takeoff away from the camera, while **(B)** shows a takeoff directed more toward the camera. **(C,D)** Relative size (standardized to the frame with the smallest grasshopper) over time in the same takeoffs as above. Size changes abruptly as the grasshopper's wings are unfurled (average relative size at 50% of the viewable grasshopper being hindwings = 2.0 ± 0.3). Note that in **(D)** size continues to rise throughout takeoff as the grasshopper jumped more toward the camera. Data were originally collected at 480 fps but shown here at 240 Hz for smoothing purposes.

TABLE 1 | Spatiotemporal characteristics of *D. carolina* escape flights.

	Takeoff	
Parameter	**Average**	**Sample size**
Time to 50% of the viewable grasshopper being hindwings (ms)	7.6 ± 1.5[a]	*n* = 8
Relative size when 50% of the visible grasshopper = hindwings	2.0 ± 0.3	*n* = 8
Time to first hindwing visibility maximum (ms)	13.5 ± 2.1	*n* = 8
Relative size at first hindwing visibility maximum	2.5 ± 0.2	*n* = 8
Brown region 10th percentile during oscillation (%)	23.2 ± 2.0	*n* = 8
Brown region 90th percentile during oscillation (%)	49.7 ± 2.3	*n* = 8
Black region 10th percentile during oscillation (%)	24.9 ± 2.3	*n* = 8
Black region 90th percentile during oscillation (%)	43.6 ± 2.1	*n* = 8
Cream region 10th percentile during oscillation (%)	22.3 ± 1.4	*n* = 8
Cream region 90th percentile during oscillation (%)	37.1 ± 2.2	*n* = 8
	Main flight	
Parameter	**Average**	**Sample size**
Wingbeat frequency (active; Hz)	31.4 ± 0.5	*n* = 14
Active wingbeat time (%)	42 ± 2	*n* = 14
Periods of active wingbeats per flight	6.1 ± 0.7	*n* = 14
Transitions between active wingbeats and pauses (transitions/sec)	6.4 ± 0.4	*n* = 14
	Landing	
Parameter	**Average**	**Sample size**
Time from 50% brown to fully brown (ms)	11.3 ± 3.0	*n* = 7[b]
Relative size from 50% brown to fully brown	0.69 ± 0.09	*n* = 7[b]
Time from last hindwing maximum to fully brown (ms)	22.7 ± 3.2	*n* = 8
Relative size from last hindwing maximum to fully brown	0.54 ± 0.09	*n* = 8
Brown 10th percentile during oscillation (%)	29.0 ± 3.1	*n* = 8
Brown 90th percentile during oscillation (%)	54.1 ± 3.2	*n* = 8
Black 10th percentile during oscillation (%)	23.7 ± 2.3	*n* = 8
Black 90th percentile during oscillation (%)	42.7 ± 2.4	*n* = 8
Cream 10th percentile during oscillation (%)	18.4 ± 2.0	*n* = 8
Cream 90th percentile during oscillation (%)	32.2 ± 2.7	*n* = 8

[a]*SEM,* [b]*one landing excluded from analysis as brown regions were never less than 50% of visible grasshopper near landing.*

Main Flight

During the main flight, grasshopper appearances changed as they alternated between periods of active wingbeats and pauses (**Figure 4** and **Table 1**). When actively beating their wings, grasshoppers showed a wingbeat frequency of 31.4 ± 0.5 Hz. Grasshoppers were actively beating their wings during 42 ± 2% of the recorded flight time (excluding final landings, see methods). Flights consisted of 6.1 ± 0.7 different periods of active wingbeats and averaged 6.4 ± 0.4 transitions between active wingbeats and pauses per second. Pauses varied in their duration and included skipping 1–2 wingbeats, shorter glides, and longer glides (**Figures 4C,D**).

Landings

Landings showed the same characteristics as takeoffs, albeit in a reverse order and at a slower speed (**Figure 5** and **Table 1**). Oscillations in the last ∼0.25 s of each flight were similar in magnitude to those seen after takeoffs (**Table 1**). The grasshopper's speed of return to all-brown (measured from 50% brown) was highly variable (min = 2.1 ms, max = 27 ms) with an average of 11.3 ± 3 ms. This was accompanied by a reduction in size to 0.69 ± 0.09 relative to when the hindwings took up 50% of the visible grasshopper.

Comparative Temporal Visual Models of Takeoff and Landing

Models examining the oscillation of colors during takeoff showed that increasingly fast visual speeds lead to greater magnitudes of oscillations in color during these time periods (**Figure 6**). Modeled values for 240 Hz vision showed significantly greater oscillations than 120 Hz vision for all three color regions (all $p < 0.01$, Student's *t*-test), and 120 Hz vision showed differences in oscillations from 60 Hz that were significantly greater than 0 (all $p < 0.01$, one-sample *t*-test).

DISCUSSION

The hindwings of *D. carolina* contrast both chromatically and achromatically when modeled through an avian visual system (**Figure 2**). Notably, the smallest region of the Carolina grasshopper's patterning—and thus likely a limiting factor in its spatial information—is the cream band with a width of 3.9 ± 0.1 mm (**Figure 1**). However, when stationary this region should be fully resolvable to a bird with modest spatial vision (10 cycles per degree; Kiltie, 2000) at distances of up to ∼4.5 m. All of these previous models ignore that the hindwings are typically only visible when in motion, and by quantifying how the visible coloration of the Carolina grasshopper changes during escape flights, we can better understand how it may be viewed by relevant predators.

During takeoff, the quick transition to this contrasting pattern may function as a deimatic defense by startling a predator. It took 7.6 ± 1.5 ms to unfurl the hindwings to 50% of the visible grasshopper, and 13.5 ± 2.1 ms for them to reach their first peak in size (**Table 1** and **Figures 3A,B**). Notably, these values would be near instantaneous to a variety of relevant observers when considering their temporal vision (human observers and non-specialist predators = CFF ∼60 Hz or 16.7 ms, Brundrett, 1974; specialist predators = CFF ∼120 Hz or 8.3 ms, Boström et al., 2016; **Figure 6**). Many studies on deimatic defenses have qualitatively noted their quick speed (**Table 2**), suggesting that speed could aid the effectiveness of startling a predator

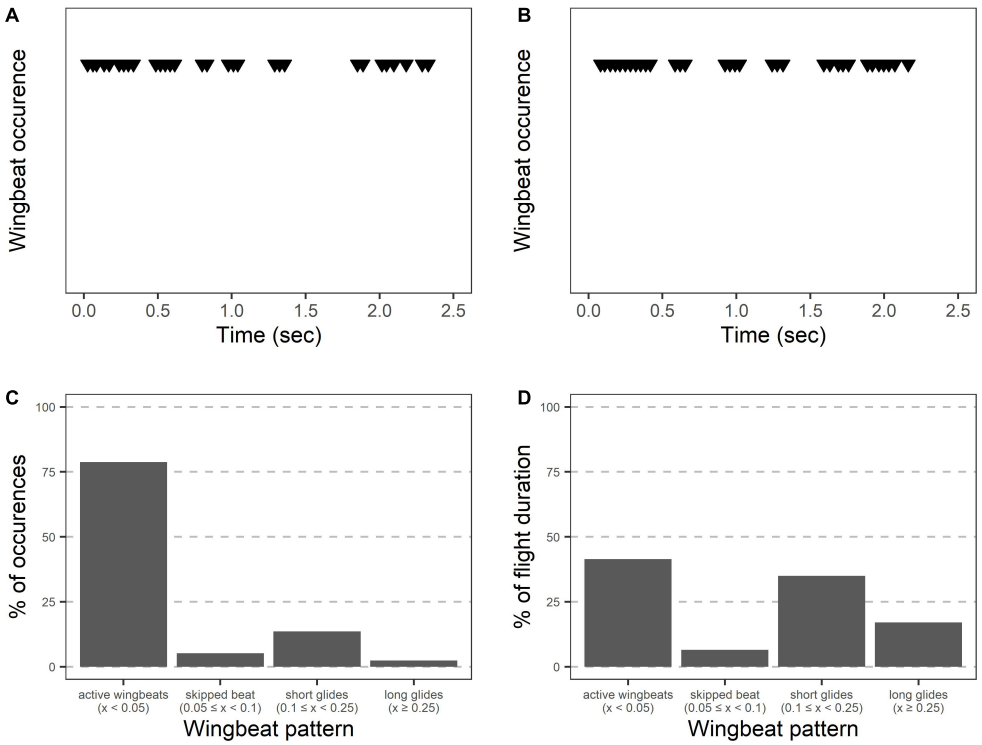

FIGURE 4 | Wingbeat patterns during Carolina grasshopper flights suggest varying appearances between active flight and gliding. **(A,B)** Two representative flights showing wingbeats over time. When actively flapping their wings, grasshoppers showed a wingbeat frequency of 31.4 ± 0.5 Hz. However, bouts of active wingbeats are interrupted by periods of gliding. Visually, grasshopper appearance would likely change between these periods due to the blurring (or lack thereof) of the wings. **(C)** Wingbeat patterns over 14 grasshopper flights. Most wingbeats occurred within 0.05 s of a previous wingbeat (representing active wingbeats), with relatively few being delayed. **(D)** However, % of time in each of the flight patterns is similar between active wingbeats (including flight while skipping 1–2 wingbeats) and periods of gliding.

(Holmes et al., 2018; Murali et al., 2019). Our quantified values are consistent with this hypothesis, as the transition takes at most two integration times even to specialized predators.

Although some deimatic displays are followed by movement (**Table 2**; Maldonado, 1970; Vallin et al., 2005; King and Adamo, 2006; Olofsson et al., 2012; Kang et al., 2017; Badiane et al., 2018), the Carolina grasshopper's is extreme as the initial transition is followed by rapid oscillations in visible colorations (**Figures 3A,B**). These oscillations represent a variety of factors (e.g., hindwing and forewing beats, changes in visual angle, forewings visibly overlapping hindwings) and typically follow no consistent pattern. These sorts of rapid, confusing changes in appearance, which have gone by a variety of names [e.g., protean defense (Humphries and Driver, 1970), dazzle camouflage (Behrens, 2012), flash display (Davis, 1948)], may work *via* disrupting the predator's search image (Humphries and Driver, 1970). Future studies could better elucidate whether these oscillations continue to aid the grasshopper *via* a deimatic defense (i.e., by startling the predator) and/or *via* disrupting the search image. Notably, the magnitudes of these oscillations increase with faster vision (**Figure 6**), making it a potential counter-adaptation for predators with quicker integration times. This would be because they would therefore perceive more of the confusing detail and potentially find it harder to follow their prey.

During the main flight, band-winged grasshoppers continued to change as a visual target. Grasshoppers alternated between periods of actively flapping their hindwings (at a frequency of 31.4 ± 0.5 Hz) and periods of gliding without wingbeats (**Figure 4** and **Table 2**). From a search image perspective, grasshoppers transition between these periods frequently (6.4 ± 0.4 transitions per second) and do not spend most of their time in just one period (active wingbeat time = 42 ± 2% of the total flight time). During the periods of active wingbeats, the grasshopper's hindwings would likely blur and/or flash to relevant observers, as an entire wing cycle would take around two integration times for viewers at 60 Hz, and four for specialized predators at 120 Hz. Conversely, glides lasted 0.19 ± 1.5 s, and therefore provided a steadier image that would contrast between active wingbeats. Dynamic changes in patterning can decrease predator accuracy in tracking and the success of capture (Humphries and Driver, 1970; Murali, 2018; Murali et al., 2019), suggesting that the wingbeat patterns of the Carolina grasshopper's main flight may serve a visual anti-predator purpose.

How quickly the hindwings disappear during landing represents a less studied—yet likely biologically important—phenomenon. Visible color regions oscillated before landing (**Figures 5A,B** and **Table 1**), at which point they returned to an all-brown appearance (time from 50% brown to fully

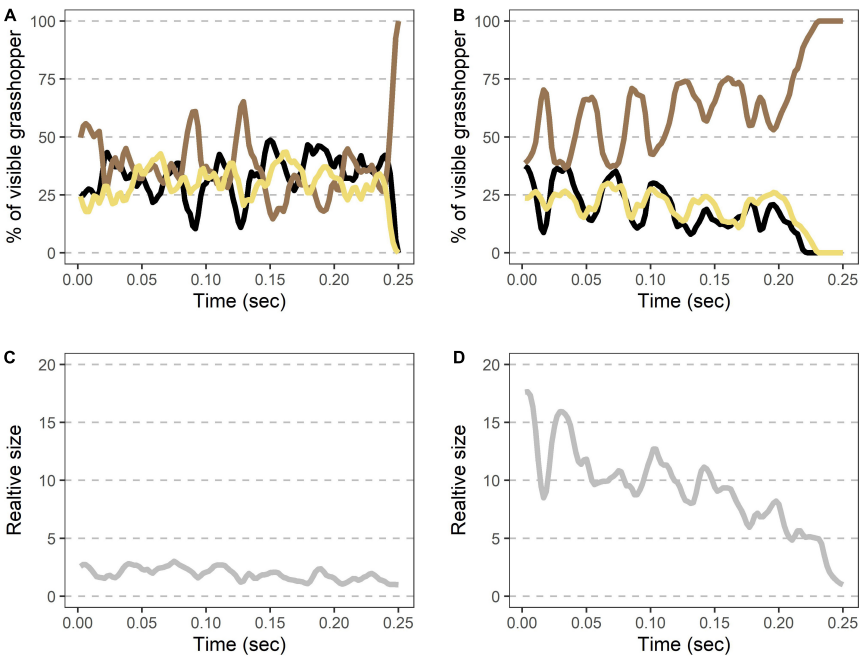

FIGURE 5 | Rapid shifts in visible color regions and size during Carolina grasshopper landings. **(A,B)** Example landings from two different flights show rapid but variable changes in visible coloration and size. **(A,B)** Percent of the visible grasshopper consisting of the three color categories brown, black, and cream. In each case, there is (1) a period of color oscillation followed by (2) a rapid return to the brown camouflaged coloration (time from 50% brown to fully brown = 11.3 ms ± 3.0). In general, the return to camouflage was slower and more variable in speed than during takeoffs. **(A)** Represents a quicker change to camouflage, while **(B)** is a more gradual landing. **(C,D)** Relative size (standardized to the frame with the smallest grasshopper) over time in the same landings as above. On average, visible grasshoppers at landing were just 54 ± 9% as large as during their last hindwing maximum. Data were originally collected at 480 fps but are shown here at 240 Hz for smoothing purposes.

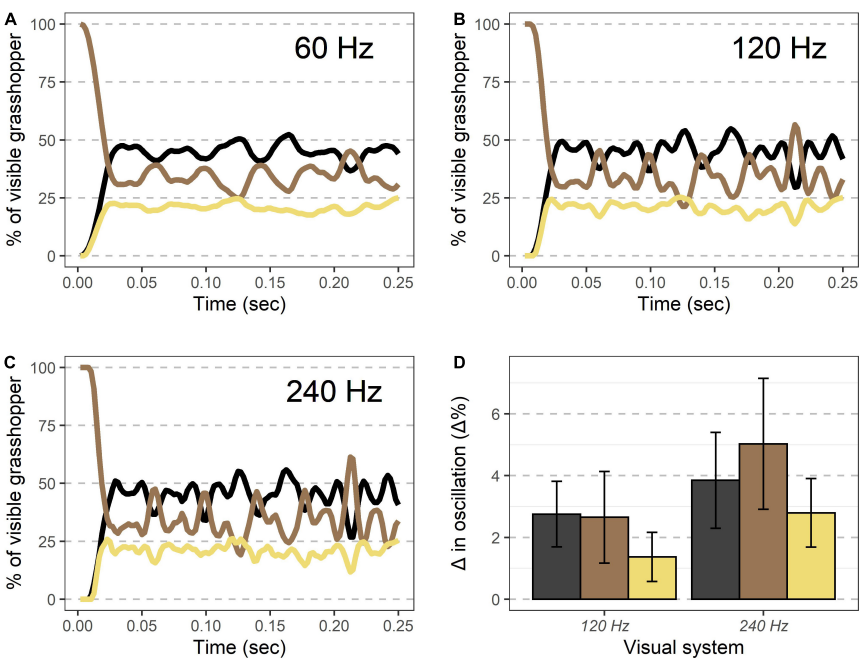

FIGURE 6 | Visible coloration shifts during takeoff modeled under different temporal visions. **(A–C)** An example takeoff of a Carolina grasshopper as seen by different visual systems. Percent of the visible grasshopper consisting of the three color categories brown, black, and cream are plotted. Compared to human vision (∼60 Hz, **A**), oscillations in coloration are more pronounced for specialist bird predators (∼120 Hz, **B**), and even more at the theoretical limit of visual speed (∼240 Hz, **C**). **(D)** Oscillation magnitude for each color (90th percentile–10th percentile for values after initial takeoff) are more pronounced in non-human visual systems for each color examined. See text for complete methods and statistics.

TABLE 2 | Temporal aspects of deimatic displays in various species.

Species	Qualitative transition speed	Quantitative transition speed	Frequency of display	Display duration	Movement after?	*n*
Northern Bluetongue skink (*Tiliqua scincoides intermedia*)[a]	"Rapid; sudden"	-	0.1–0.2/sec	-	Yes	13
Spotted lanternfly (*Lycorma delicatula*)[b]	"Sudden"	-	-	15.16 ± 1.71 secs	Yes	91
Stagmatoptera biocellata[c]	"Violent; dramatic"	-	-	Typically 2–45 min	Yes	20
Large brown mantis (*Archimantis latistyla*)[d]	"Sudden"	-	-	-	-	35
Giant rainforest mantis (*Hierodula majuscula*)[d]	"Sudden"	-	-	-	-	20
False garden mantis (*Pseudomantis albofimbriata*)[d]	"Sudden"	-	-	-	-	25
European swallowtail butterfly (*Papilio machaon*)[e]	"Sudden"	-	Up to 0.3/min	-	Yes	27
Mountain katydid (*Acripeza reticulata*)[f]	"Sudden"	-	-	≤ 300 s	-	32
Peacock butterfly (*Inachis io*)[g]	"Sudden"	-	< 2/min	-	Yes	54
Common cuttlefish (*Sepia officinalis*)[h]	"Rapid; sudden"	-	-	3–12 s	Yes	6
Ringneck snake (*Diadophis punctatus*)[i]	"Sudden"	-	-	-	No	25

[a]*Badiane et al. (2018)*, [b]*Kang et al. (2017)*, [c]*Maldonado (1970)*, [d]*O'Hanlon et al. (2018)*, [e]*Olofsson et al. (2012)*, [f]*Umbers and Mappes (2015)*, [g]*Vallin et al. (2005)*, [h]*King and Adamo (2006)*, [i]*Cox et al. (2021)*.

brown = 11.3 ± 3.0 ms) while simultaneously reducing their overall size (**Figures 5C,D**). The speed of this return was slower than the transition during takeoff and varied considerably between individuals (compare **Figure 5A** vs. **Figure 5B**). This could be due to some grasshoppers requiring more control when landing on certain surfaces. However, specialized predators would still only be able to form, at most, around four images of the transition before their prey returned to an all-brown appearance, which as Cooper (2006) suggested, may cause "predators [to] misjudge the landing site." Therefore, this quick disappearance of a highly contrasting region may constitute a third interwoven phase in the escape strategy of the Carolina grasshopper, alongside deimatic and protean defenses. If so, this bears a resemblance to the blanch-ink-jet behavior of longfin squid, in which the squid turns clear to hide itself, and then uses an ink cloud to confuse and/or startle predators as it flees, thereby similarly combining a transition with deimatic/protean defenses (Staudinger et al., 2011). Notably in the Carolina grasshopper, landing occurs last within this sequence, so its effectiveness may depend on the distances created by prior defenses.

Our simplistic measurements of color in this system likely represent an underestimate of its true temporal variability. We categorized color into three categories because Carolina grasshopper coloration is fairly distinct between body regions and consistent within them (e.g., **Figures 1**, **2**). However, a predator's perception of the grasshopper is also dependent on other factors, including both environmental and physiological properties. Environmentally, the variability of color and patterning in flight would be increased by changes in illumination (Endler, 1993) or angular dependence of reflection (Stuart-Fox et al., 2021). Physiologically, our measurements do not account for the spatiotemporal variation of where these different colorations are located, and thus their interactions with predator vision (Hughes, 1977; Smolka and Hemmi, 2009). As technology improves, future studies could account for all these factors simultaneously. However, we feel that our simplified color measurements provide a biologically relevant and feasible step in characterizing variation at these temporal resolutions.

Furthermore, the appearance of Carolina grasshoppers to their avian predators will not be identical to our experience watching these videos because of differences in visual umwelt, distance, and angle of view. Avian color vision is both tetrachromatic and refined *via* the presence of oil droplets (Bowmaker et al., 1997; Hart and Vorobyev, 2005). As a result, their perception of hindwing color differs from ours, although it is still highly contrasting because of the dark and bright hindwing regions (**Figure 2**). Additionally, excluding birds of prey, many birds have coarser spatial vision than our own, which may blur some of the patterning (Caves et al., 2018). This combined with uncertainty in the distance from the bird to the grasshopper during pursuit could lead to different outcomes of colors blending or being seen as distinct. Lastly, an avian predator may approach from an angle that differs from our camera, and pursuit may change this angle. Differences in angle can lead to varying visual scenes (e.g., Cummings et al., 2008; Brandley et al., 2016), and future work should thoroughly investigate this phenomenon in a more natural context.

At the evolutionary level, the hindwings of band-winged grasshoppers present an interesting case study of how a single structure may be under multiple different selective pressures. In addition to their anti-predator purposes and inherent biomechanical function, hindwings may also serve in visual conspecific signaling (Otte, 1970, 1985; although behavioral data is lacking). Hindwing patterning often varies. between species of band-winged grasshoppers, including in areas of transparency, placement of the band, hue, and likely in achromatic properties. Notably, transparent regions, which some other band-winged species possess (**Figure 1C**), could allow for differences between the biomechanical and visual properties of the wings, and the coarse visual acuity of band-winged grasshoppers (Horridge, 1978; Krapp and Gabbiani, 2005; Duncan et al., 2021) may make fine-scale patterning less important for conspecific signaling than for anti-predator purposes. Differences in color vision may also

play a role, with some species lacking a long-wavelength receptor (Vishnevskaya and Shura-Bura, 1990; Schmeling et al., 2014). However, in order to study why hindwing patterning varies between species, researchers will need to understand how these structures move in nature, and how this motion may be viewed by relevant receivers.

By quantifying the speed of visible pattern change in our study, we have begun to infer how these escape flights may appear to observers with differing temporal visual systems. Work in other visual parameters such as color vision (Endler, 1980; Cummings et al., 2003; Brandley et al., 2013) and visual acuity (Melin et al., 2016; Caves et al., 2018) has demonstrated the necessity of viewing natural phenomena through the eyes of relevant receivers. Therefore, when considering the differences in temporal vision across species (Healy et al., 2013), future studies must quantify natural motion patterns rather than relying on the human experience.

DATA AVAILABILITY STATEMENT

The original contributions presented in this study are included in the article/**Supplementary Material**, further inquiries can be directed to the corresponding author.

AUTHOR CONTRIBUTIONS

EM and NB conceptualized the project, performed the data analysis, and wrote the first draft of the manuscript. NB acquired funding. EM collected all videos from the field and scored all takeoffs and landings. SB and HS scored all main flight videos. FG performed all spectrometry including collection of grasshoppers. All authors contributed to the article and approved the submitted version.

FUNDING

HS was supported by the College of Wooster's Sophomore Research Program. Funds for equipment came from the College of Wooster's Start-up Grant to NB.

ACKNOWLEDGMENTS

We thank Teddi Farson, Cameron Papp, and Christa Zianni for support in the field, Brae Salazar for photos of band-winged grasshopper hindwings, and Michael Rosario for consultation regarding high-speed video options.

SUPPLEMENTARY MATERIAL

The Supplementary Material for this article can be found online at: https://www.frontiersin.org/articles/10.3389/fevo.2022.900544/full#supplementary-material

REFERENCES

Badiane, A., Carazo, P., Price-Rees, S. J., Ferrando-Bernal, M., and Whiting, M. J. (2018). Why blue tongue? A potential UV-based deimatic display in a lizard. *Behav. Ecol. Sociobiol.* 72:104. doi: 10.1007/s00265-018-2512-8

Barthelmé, S., and Tschumperlé, D. (2019). Imager: an R package for image processing based on CImg. *J. Open Source Softw.* 4:1012. doi: 10.21105/joss.01012

Behrens, R. R. (2012). *Ship Shape, a Dazzle Camouflage Sourcebook*. Dysart, IA: Bobolink Books.

Belovsky, G. E., and Slade, J. B. (1993). The role of vertebrate and invertebrate predators in a grasshopper community. *Oikos* 68, 193–201. doi: 10.2307/3544830

Boström, J. E., Dimitrova, M., Canton, C., Håstad, O., Qvarnström, A., and Ödeen, A. (2016). Ultra-rapid vision in birds. *PLoS One* 11:e0151099. doi: 10.1371/journal.pone.0151099

Bowmaker, J. K., Health, L. A., Wilkie, S. E., and Hunt, D. M. (1997). Visual pigments and oil droplets from six classes of photoreceptor in the retinas of birds. *Vision Res.* 37, 2183–2194. doi: 10.1016/S0042-6989(97)00026-6

Brandley, N., Johnson, M., and Johnsen, S. (2016). Aposematic signals in North American black widows are more conspicuous to predators than to prey. *Behav. Ecol.* 27, 1104–1112. doi: 10.1093/beheco/arw014

Brandley, N. C., Speiser, D. I., and Johnsen, S. (2013). Eavesdropping on visual secrets. *Evol. Ecol.* 27, 1045–1068. doi: 10.1007/s10682-013-9656-9

Brundrett, G. W. (1974). Human sensitivity to flicker. *Light. Res. Technol.* 6, 127–143. doi: 10.1177/096032717400600302

Caves, E. M., Brandley, N. C., and Johnsen, S. (2018). Visual acuity and the evolution of signals. *Trends Ecol. Evol.* 33, 358–372. doi: 10.1016/j.tree.2018.03.001

Cooper, W. E. (2006). Risk factors and escape strategy in the grasshopper *Dissosteira carolina*. *Behaviour* 143, 1201–1218.

Cox, C. L., Chung, A. K., Blackwell, C., Davis, M. M., Gulsby, M., Islam, H., et al. (2021). Tactile stimuli induce deimatic antipredator displays in ringneck snakes. *Ethology* 127, 465–474. doi: 10.1111/eth.13152

Cummings, M. E., Jordão, J. M., Cronin, T. W., and Oliveira, R. F. (2008). Visual ecology of the fiddler crab, Uca tangeri: effects of sex, viewer and background on conspicuousness. *Anim. Behav.* 75, 175–188. doi: 10.1016/j.anbehav.2007.04.016

Cummings, M. E., Rosenthal, G. G., and Ryan, M. J. (2003). A private ultraviolet channel in visual communication. *Proc. Biol. Sci.* 270, 897–904. doi: 10.1098/rspb.2003.2334

Davis, D. D. (1948). Flash display of aposematic colors in *Farancia* and other snakes. *Copeia* 1948, 208–211. doi: 10.2307/1438456

Donner, K. (2021). Temporal vision: measures, mechanisms and meaning. *J. Exp. Biol.* 224:jeb222679. doi: 10.1242/jeb.222679

Duncan, A. B., Salazar, B. A., Garcia, S. R., and Brandley, N. C. (2021). A sexual dimorphism in the spatial vision of North American band-winged grasshoppers. *Integr. Comp. Biol.* 3:obab008. doi: 10.1093/iob/obab008

Endler, J. A. (1980). Natural selection on color patterns in *Poecilia reticulata*. *Evolution* 34, 76–91. doi: 10.2307/2408316

Endler, J. A. (1993). The color of light in forests and its implications. *Ecol. Monogr.* 63, 1–27. doi: 10.2307/2937121

Girard, M. B., Kasumovic, M. M., Elias, D. O., and Dyer, A. G. (2011). Multi-modal courtship in the peacock spider, Maratus volans (O.P.-Cambridge, 1874). *PLoS One* 6:e25390. doi: 10.1371/journal.pone.0025390

Hall, J. R., Cuthill, I. C., Baddeley, R., Shohet, A. J., and Scott-Samuel, N. E. (2013). Camouflage, detection and identification of moving targets. *Proc. Biol. Sci.* 280:20130064. doi: 10.1098/rspb.2013.0064

Hart, N. S. (2001). The visual ecology of avian photoreceptors. *Prog. Retin. Eye Res.* 20, 675–703. doi: 10.1016/S1350-9462(01)00009-X

Hart, N. S., and Vorobyev, M. (2005). Modelling oil droplet absorption spectra and spectral sensitivities of bird cone photoreceptors. *J. Comp. Physiol.* 191, 381–392. doi: 10.1007/s00359-004-0595-3

Healy, K., McNally, L., Ruxton, G. D., Cooper, N., and Jackson, A. L. (2013). Metabolic rate and body size are linked with perception of temporal information. *Anim. Behav.* 86, 685–696. doi: 10.1016/j.anbehav.2013.06.018

Holmes, G. G., Delferrière, E., Rowe, C., Troscianko, J., and Skelhorn, J. (2018). Testing the feasibility of the startle-first route to deimatism. *Sci. Rep.* 8:10737. doi: 10.1038/s41598-018-28565-w

Horridge, G. A. (1978). The separation of visual axes in apposition compound eyes. *Philos. Trans. R. Soc. Lond. B Biol. Sci.* 285, 1–59. doi: 10.1098/rstb.1978.0093

How, M. J., and Zanker, J. M. (2014). Motion camouflage induced by zebra stripes. *Zoology* 117, 163–170. doi: 10.1016/j.zool.2013.10.004

Hughes, A. (1977). "The Topography of Vision in Mammals of Contrasting Life Style: Comparative Optics and Retinal Organisation," in *The Visual System in Vertebrates*, eds F. Crescitelli, C. A. Dvorak, D. J. Eder, A. M. Granda, D. Hamasaki, K. Holmberg, et al. (Berlin: Springer), 613–756.

Humphries, D. A., and Driver, P. M. (1970). Protean defence by prey animals. *Oecologia* 5, 285–302. doi: 10.1007/BF00815496

Ioannou, C. C., and Krause, J. (2009). Interactions between background matching and motion during visual detection can explain why cryptic animals keep still. *Biol. Lett.* 5, 191–193. doi: 10.1098/rsbl.2008.0758

Jackson, J. F., Ingram, W., and Campbell, H. W. (1976). The dorsal pigmentation pattern of snakes as an antipredator strategy: a multivariate approach. *Am. Nat.* 110, 1029–1053. doi: 10.1086/283125

Kang, C., Moon, H., Sherratt, T. N., Lee, S., and Jablonski, P. G. (2017). Multiple lines of anti-predator defence in the spotted lanternfly, *Lycorma delicatula* (Hemiptera: Fulgoridae). *Biol. J. Linn. Soc.* 120, 115–124. doi: 10.1111/bij.12847

Kiltie, R. A. (2000). Scaling of visual acuity with body size in mammals and birds. *Funct. Ecol.* 14, 226–234. doi: 10.1046/j.1365-2435.2000.00404.x

King, A. J., and Adamo, S. A. (2006). The ventilatory, cardiac and behavioural responses of resting cuttlefish (*Sepia officinalis* L.) to sudden visual stimuli. *J. Exp. Biol.* 209, 1101–1111. doi: 10.1242/jeb.02116

Krapp, H. G., and Gabbiani, F. (2005). Spatial distribution of inputs and local receptive field properties of a wide-field, looming sensitive neuron. *J. Neurophysiol.* 93, 2240–2253. doi: 10.1152/jn.00965.2004

Laan, A., Gutnick, T., Kuba, M. J., and Laurent, G. (2014). Behavioral analysis of cuttlefish traveling waves and its implications for neural control. *Curr. Biol.* 24, 1737–1742. doi: 10.1016/j.cub.2014.06.027

Maia, R., Gruson, H., Endler, J. A., and White, T. E. (2019). pavo 2: new tools for the spectral and spatial analysis of colour in R. *Methods Ecol. Evol.* 10, 1097–1107. doi: 10.1111/2041-210X.13174

Maldonado, H. (1970). The deimatic reaction in the praying mantis *Stagmatoptera biocellata*. *Z. Vergl. Physiol.* 68, 60–71. doi: 10.1007/BF00297812

Mather, J. A., and Mather, D. L. (2004). Apparent movement in a visual display: the 'passing cloud' of *Octopus cyanea* (Mollusca: Cephalopoda). *J. Zool.* 263, 89–94. doi: 10.1017/S0952836904004911

Melin, A. D., Kline, D. W., Hiramatsu, C., Caro, T., and Osorio, D. (2016). Zebra stripes through the eyes of their predators, zebras, and humans. *PLoS One* 11:e0145679. doi: 10.1371/journal.pone.0145679

Murali, G. (2018). Now you see me, now you don't: dynamic flash coloration as an antipredator strategy in motion. *Anim. Behav.* 142, 207–220. doi: 10.1016/j.anbehav.2018.06.017

Murali, G., Kumari, K., and Kodandaramaiah, U. (2019). Dynamic colour change and the confusion effect against predation. *Sci. Rep.* 9:274. doi: 10.1038/s41598-018-36541-7

O'Hanlon, J. C., Rathnayake, D. N., Barry, K. L., and Umbers, K. D. L. (2018). Post-attack defensive displays in three praying mantis species. *Behav. Ecol. Sociobiol.* 72:176. doi: 10.1007/s00265-018-2591-6

Olofsson, M., Eriksson, S., Jakobsson, S., Wiklund, C., and Osorio, D. (2012). Deimatic display in the European swallowtail butterfly as a secondary defence against attacks from great tits. *PLoS One* 7:e47092. doi: 10.1371/journal.pone.0047092

Olofsson, M., Løvlie, H., Tibblin, J., Jakobsson, S., and Wiklund, C. (2013). Eyespot display in the peacock butterfly triggers antipredator behaviors in naïve adult fowl. *Behav. Ecol.* 24, 305–310. doi: 10.1093/beheco/ars167

Ord, T. J., and Stamps, J. A. (2008). Alert signals enhance animal communication in "noisy" environments. *Proc. Natl. Acad. Sci. U.S.A.* 105, 18830–18835. doi: 10.1073/pnas.0807657105

Otte, D. (1970). A comparative study of communicative behavior in grasshoppers. *Misc. Pub. Mus. Zool. Univ. Mich.* 141, 1–169.

Otte, D. (1985). *The North American Grasshoppers*, Vol. 2. Cambridge, MA: Harvard UP.

Peters, R. A., Hemmi, J. M., and Zeil, J. (2007). Signaling against the wind: modifying motion-signal structure in response to increased noise. *Curr. Biol.* 17, 1231–1234. doi: 10.1016/j.cub.2007.06.035

Ruxton, G. D., Allen, W. L., Sherratt, T. N., and Speed, M. P. (2018). *Avoiding Attack: The Evolutionary Ecology of Crypsis, Aposematism, and Mimicry*. Oxford: Oxford University Press.

Schmeling, F., Wakakuwa, M., Tegtmeier, J., Kinoshita, M., Bockhorst, T., Arikawa, K., et al. (2014). Opsin expression, physiological characterization and identification of photoreceptor cells in the dorsal rim area and main retina of the desert locust, Schistocerca gregaria. *J. Exp. Biol.* 217, 3557–3568. doi: 10.1242/jeb.108514

Schneider, C. A., Rasband, W. S., and Eliceiri, K. W. (2012). NIH Image to ImageJ: 25 years of image analysis. *Nat. Methods* 9, 671–675. doi: 10.1038/nmeth.2089

Smolka, J., and Hemmi, J. M. (2009). Topography of vision and behaviour. *J. Exp. Biol.* 212, 3522–3532. doi: 10.1242/jeb.032359

Staudinger, M. D., Hanlon, R. T., and Juanes, F. (2011). Primary and secondary defences of squid to cruising and ambush fish predators: variable tactics and their survival value. *Anim. Behav.* 81, 585–594. doi: 10.1016/j.anbehav.2010.12.002

Stoddard, M. C., and Prum, R. O. (2008). Evolution of avian plumage coloration in a tetrahedral color space: a phylogenetic analysis of new world buntings. *Am. Nat.* 171, 755–776. doi: 10.1086/587526

Stuart-Fox, D., Ospina-Rozo, L., Ng, L., and Franklin, A. M. (2021). The paradox of iridescent signals. *Trends Ecol. Evol.* 36, 187–195. doi: 10.1016/j.tree.2020.10.009

Tan, E. J., and Elgar, M. A. (2021). Motion: enhancing signals and concealing cues. *Biol. Open* 10: bio058762. doi: 10.1242/bio.058762

Umbers, K. D. L., Lehtonen, J., and Mappes, J. (2015). Deimatic displays. *Curr. Biol.* 25, R58–R59. doi: 10.1016/j.cub.2014.11.011

Umbers, K. D. L., and Mappes, J. (2015). Postattack deimatic display in the mountain katydid, Acripeza reticulata. *Anim. Behav.* 100, 68–73. doi: 10.1016/j.anbehav.2014.11.009

Umeton, D., Read, J. C. A., and Rowe, C. (2017). Unravelling the illusion of flicker fusion. *Biol. Lett.* 13:20160831. doi: 10.1098/rsbl.2016.0831

Vallin, A., Jakobsson, S., Lind, J., and Wiklund, C. (2005). Prey survival by predator intimidation: an experimental study of peacock butterfly defence against blue tits. *Proc. Biol. Sci.* 272, 1203–1207. doi: 10.1098/rspb.2004.3034

Vishnevskaya, T. M., and Shura-Bura, T. M. (1990). "Spectral Sensitivity of Photoreceptors and Spectral Inputs to the Neurons of the First Optic Ganglion in the Locust (Locusta migratoria)," in *Sensory Systems and Communication in Arthropods*, eds F. G. Gribakin, K. Wiese, and A. V. Popov (Basel: Birkhäuser), 106–111.

Vorobyev, M., Osorio, D., Bennett, A., Marshall, N., and Cuthill, I. (1998). Tetrachromacy, oil droplets and bird plumage colours. *J. Comp. Physiol. A Neuroethol. Sens. Neural. Behav. Physiol.* 183, 621–633. doi: 10.1007/s003590050286

Wickham, H. (2016). *ggplot2: Elegant Graphics for Data Analysis*. New York, NY: Springer-Verlag.

Conflict of Interest: The authors declare that the research was conducted in the absence of any commercial or financial relationships that could be construed as a potential conflict of interest.

Publisher's Note: All claims expressed in this article are solely those of the authors and do not necessarily represent those of their affiliated organizations, or those of the publisher, the editors and the reviewers. Any product that may be evaluated in this article, or claim that may be made by its manufacturer, is not guaranteed or endorsed by the publisher.